

UC Irvine

UC Irvine Previously Published Works

Title

Early-life febrile seizures worsen adult phenotypes in Scn1a mutants

Permalink

<https://escholarship.org/uc/item/2d6880qf>

Authors

Dutton, Stacey BB

Dutt, Karoni

Papale, Ligia A

et al.

Publication Date

2017

DOI

10.1016/j.expneurol.2017.03.026

Copyright Information

This work is made available under the terms of a Creative Commons Attribution License, available at <https://creativecommons.org/licenses/by/4.0/>

Peer reviewed



Research Paper

Early-life febrile seizures worsen adult phenotypes in *Scn1a* mutantsStacey B.B. Dutton^{a,d}, Karoni Dutt^b, Ligia A. Papale^a, Sandra Helmers^c, Alan L. Goldin^b, Andrew Escayg^{a,*}^a Department of Human Genetics, Emory University, Atlanta, GA 30022, USA^b Departments of Microbiology & Molecular Genetics and Anatomy & Neurobiology, University of California, Irvine, CA 92697, USA^c Department of Neurology, Emory University, Atlanta, GA 30022, USA^d Department of Biology, Agnes Scott College, Atlanta, GA 30030, USA

ARTICLE INFO

Article history:

Received 15 September 2016

Received in revised form 17 February 2017

Accepted 22 March 2017

Available online 1 April 2017

Keywords:

Febrile seizures

GEFS+

SCN1A

Epilepsy

Na_v1.1

ABSTRACT

Mutations in the voltage-gated sodium channel (VGSC) gene *SCN1A*, encoding the Na_v1.1 channel, are responsible for a number of epilepsy disorders including genetic epilepsy with febrile seizures plus (GEFS+) and Dravet syndrome (DS). Patients with *SCN1A* mutations often experience prolonged early-life febrile seizures (FSs), raising the possibility that these events may influence epileptogenesis and lead to more severe adult phenotypes. To test this hypothesis, we subjected 21–23-day-old mice expressing the human *SCN1A* GEFS+ mutation R1648H to prolonged hyperthermia, and then examined seizure and behavioral phenotypes during adulthood. We found that early-life FSs resulted in lower latencies to induced seizures, increased severity of spontaneous seizures, hyperactivity, and impairments in social behavior and recognition memory during adulthood. Biophysical analysis of brain slice preparations revealed an increase in epileptiform activity in CA3 pyramidal neurons along with increased action potential firing, providing a mechanistic basis for the observed worsening of adult phenotypes. These findings demonstrate the long-term negative impact of early-life FSs on disease outcomes. This has important implications for the clinical management of this patient population and highlights the need for therapeutic interventions that could ameliorate disease progression.

© 2017 Elsevier Inc. All rights reserved.

1. Introduction

Febrile seizures (FSs) are convulsions triggered by high fever. They are the most common type of pediatric seizure, affecting 2–5% of children between 6 months and 5 years of age in the United States (Shinnar and Glauser, 2002). Retrospective studies of resected brain tissue from adults with temporal lobe epilepsy (TLE) suggest a strong correlation between the development of TLE and early-life FSs (Falconer et al., 1964; French et al., 1993). In addition, studies conducted by Cendes et al. (1993) found that the prevalence of TLE exhibiting mesial temporal sclerosis is higher in patients with a history of complex early-life FSs. However, these studies did not establish whether the development of epilepsy was a consequence of the early-life FSs or a manifestation of the disease presentation.

Familial and twin studies have shown that genetic factors contribute significantly to the etiology of FSs (Rich et al., 1987; Tsuboi, 1987; Tsuboi and Endo, 1991), and recent studies have uncovered at least 12 loci associated with FSs (Reviewed in Feng and Chen, 2016). Mutations in *SCN1A*, the gene encoding the α -subunit of the Na_v1.1 voltage-gated sodium channel, are responsible for several epilepsy disorders,

including genetic epilepsy with febrile seizures plus (GEFS+) and Dravet syndrome (DS). GEFS+ is characterized by FSs that sometimes persist beyond 6 years of age, as well as the development of a range of epilepsy subtypes, including generalized tonic clonic (GTCS) and myoclonic seizures (Scheffer and Berkovic, 1997). DS is a severe childhood epileptic encephalopathy characterized by frequent and complex FSs beginning in the first year of life, afebrile generalized seizures, cognitive and behavioral deficits, and ataxia (Mullen and Scheffer, 2009). The occurrence of early-life FSs in these disorders demonstrates that altered *SCN1A* function increases susceptibility to FSs and raises the possibility that these early-life events may influence disease progression.

Evidence for the long-term negative effects of early-life prolonged FSs has been derived from experiments on rodent pups. By exposing 10–12-day old rat pups to a stream of heated air for 30 min, Baram et al. (1997) demonstrated that hyperthermia can be used to model febrile seizure events. The seizures produced in that paradigm resulted in increased inhibitory presynaptic transmission in the adult hippocampus (Chen et al., 1999) and transient cell injury (Toth et al., 1998; Bender et al., 2003). Dube et al. (2006) subsequently showed that P10 rat pups subjected to prolonged hyperthermia develop spontaneous seizures of hippocampal origin around 3 months of age. In addition, early-life FSs have been associated with a range of biological changes including increased IL-1 β production (Matsuo et al., 2006; Feng and Chen, 2016), altered expression of hyperpolarization activated cyclic

* Corresponding author at: Emory University, Department of Human Genetics, 615 Michael Street, Whitehead Building, Suite 301, Atlanta, GA 30322, USA.

E-mail address: aescayg@emory.edu (A. Escayg).

nucleotide-gated (HCN) channels (Chen et al., 2001; Brewster et al., 2002; Brewster et al., 2005), reduced number of astrocyte gap junctions in the hippocampus (Brewster et al., 2005), motor map reorganization (Reid et al., 2012), enhanced GABA_A and benzodiazepine receptor binding (Gonzalez Ramirez et al., 2007), reduced expression of GABA_B receptor subunits (Han et al., 2006), and altered expression of genes involved in stress, inflammation, glial activation, and myelination (Jongbloets et al., 2015). Taken together, these studies demonstrate the early-life FSs can have long-term pro-epileptic effects in developing rodents. However, it was unknown whether these alterations would be exacerbated in the presence of a *SCN1A* mutation. A better understanding of the relationship between early-life FSs and the development of epilepsy in *SCN1A*-derived disorders will provide insight into the epileptogenic process and may identify new opportunities for therapeutic intervention.

To investigate the impact of early-life FSs on the development of *SCN1A*-derived epilepsy, we first examined the effect of age on susceptibility to hyperthermia-induced seizures in mice expressing the human *SCN1A* GEFS+ mutation R1648H (*RH*). Next, we used the mutant mice to explore the effect of prolonged and recurrent early-life FSs on adult phenotypes. We found that early-life FSs were associated with an increase in seizure susceptibility and spontaneous seizure severity, hyperactivity, and impairments in social behaviors and recognition memory in the adult mutants. Current-clamp recordings from hippocampal slices of the mutant mice that experienced early-life FSs showed increased firing of action potentials (AP) in pyramidal neurons. We also saw increased epileptiform activity in pyramidal neurons of mutants that experienced early-life FSs. These findings argue for the clinical benefit of preventing fevers in infants who have *SCN1A* mutations and highlight the need for therapeutic interventions to ameliorate the long-term consequences of early-life prolonged FSs.

2. Materials and methods

2.1. Animals

The mouse line expressing the human *SCN1A* R1648H GEFS+ mutation (*RH* line) was generated as we previously described (Martin et al., 2010) and is maintained on the C57BL/6J background. Wild-type (WT) littermates were used as controls for all experiments to minimize variation due to differences in genetic background and rearing conditions. Mice were housed on a 12-h light/dark cycle with food and water available ad libitum. All experiments were conducted at the N4 backcross generation. All experiments involving mice were performed in accordance with the guidelines of the Institutional Animal Care and Use Committees of Emory University and the University of California, Irvine.

2.2. Acute hyperthermia seizure induction

Susceptibility to hyperthermia-induced seizures (a model of febrile seizure susceptibility) was determined as previously described (Dutton et al., 2013). Male and female mice were previously found to respond similarly to hyperthermia, therefore data from both sexes were combined. Heterozygous (*RH/+*), homozygous (*RH/RH*), and WT littermates were evaluated at 3 ages: P14–15 (WT - Males: 4, Females: 4; *RH/+* - Males: 4, Females: 4; *RH/RH* - Males: 2, Females: 3), P22–24 (WT - Males: 4, Females: 4; *RH/+* - Males: 4, Females: 4; *RH/RH* - Males: 3, Females: 3), and P32–33 (WT - Males: 5, Females: 4; *RH/+* - Males: 4, Females: 5). Each mouse was tested only once. Briefly, each mouse was placed in a Plexiglas tube and fitted with a rectal temperature probe connected to a heating lamp via a temperature controller (TCAT 2DF, Physitemp). The mouse was held at 37.5 °C for 30 min to acclimatize to the chamber and to obtain baseline electroencephalographic (EEG) activity. Body temperature was then elevated by 0.5 °C every 2 min until a seizure occurred or a maximum temperature of 42.5 °C

was reached. Seizure behaviors were scored using a modified Racine scale: 1, staring; 2, head nodding; 3, unilateral forelimb clonus; 4, bilateral forelimb clonus; 5, rearing and falling; 6, clonic seizure involving loss of postural control with rapid movement in all 4 limbs. Seizure induction was coupled with real-time video/EEG recordings for each mouse.

2.3. Models of complex early-life FS events

Two different paradigms were developed to investigate the long-term effects of complex early-life FSs. *RH/+* mice and WT littermates (P22–23) were used for both paradigms.

(1) Prolonged febrile event (PFE)

The PFE paradigm was used to model an early-life prolonged febrile seizure event. Each mouse was placed in a Plexiglas cylinder and fitted with a rectal temperature probe connected to a heating lamp via a temperature controller. Mouse core body temperature was held at 37.5 °C for 10 min, allowing the mouse to acclimatize to the chamber. Core body temperature was elevated by 0.5 °C every 2 min until 41.5 °C was reached, and this core body temperature was then maintained for 30 min. The core body temperature at the occurrence of each seizure as well as the total number of seizures and the severity of each seizure (as measured on the modified Racine scale) were noted for each mouse. The mouse was then transferred to its home cage, and no further procedures were performed for 2 months. Mutants and WT littermates that were handled similarly but not exposed to external heat via the heat lamp were used as controls. In a separate cohort of mice ($n = 4–5$ per genotype), febrile seizure induction was coupled with real-time video/EEG recordings to confirm behavioral seizures.

(2) Acute/prolonged febrile event (A/PFE)

The A/PFE paradigm was used to model recurrent FSs in which an acute febrile seizure is subsequently followed by a prolonged febrile seizure event. On the first day, the mouse was held at 37.5 °C for 10 min to acclimatize to the chamber. Body temperature was then elevated by 0.5 °C every 2 min until a seizure occurred or a maximum temperature of 42.5 °C was reached. The mouse was then returned to its home cage. On the following day (18–24 h later), the mouse was held at 37.5 °C for 10 min, and then its core body temperature was elevated by 0.5 °C every 2 min until 41.5 °C was reached. Core body temperature was maintained at 41.5 °C for 30 min and the observed seizures were scored as described above. The mouse was then returned to its home cage and no further procedures were performed for 2 months. WT and *RH/+* mice that were handled similarly but not exposed to the external heat served as controls.

2.4. Flurothyl seizure induction

Thresholds to flurothyl-induced seizures were determined as we previously described (Martin et al., 2010). Two months after the PFE or A/PFE, mice (P82) were exposed to flurothyl (2,2,2-trifluoroethylether, Sigma) at a rate of 20 μ l/min. Latencies to the first myoclonic jerk (MJ), the first generalized tonic clonic seizure (GTCS), and the generalized tonic clonic seizure with hindlimb extension (HE) were determined. A total of 16 WT controls (males: 8, females: 8), 15 *RH/+* controls (males: 9, females: 6), 16 PFE WT (males: 8, females: 8), and 14 PFE *RH/+* (males: 7, females: 7) were examined for the PFE paradigm. For the A/PFE paradigm, a total of 15 WT controls (males: 9, females: 6), 15 *RH/+* controls (males: 9, females: 6), 16 A/PFE WT (males: 8, females: 8), and 14 A/PFE *RH/+* (males: 7, females: 7) were examined.

2.5. EEG surgery and real-time video/EEG acquisition during FS induction

Heterozygous *RH/+* mice and WT littermates (P14–15, P22–24, and P32–33; $n = 8$ –9 per genotype, 3–4 males/group; 4–5 females/group) were anesthetized with isoflurane and surgically implanted with 2 pairs of sterile stainless steel screw electrodes (0.10 in. in diameter; Pinnacle Technology, Inc.). The first pair of electrodes was placed posterior to Bregma in the right hemisphere (EEG₁ and EEG₂), and the second pair of electrodes was placed at the corresponding positions in the left hemisphere (EEG₃ and EEG₄). Following electrode placement, fine wires were wrapped tightly around each screw and dental acrylic was applied. Following 2 h of recovery from surgery, each mouse was subjected to febrile seizure induction and real-time video and EEG signals were collected, processed, and digitized at a sampling rate of 200 Hz by the Stellate Harmonie amplifier and software (Natus Medical, Inc., CA). Additional details on the EEG acquisition and analysis are provided as Supplementary Data. No statistically significant differences were observed between sexes; therefore, male and female data were combined.

2.6. Immunohistochemistry for *c-Fos* reactivity

c-Fos immunoreactivity was evaluated 2 h after the acute hyperthermia-induced seizure in male *RH/+* mutants and in WT littermates that were similarly handled ($n = 8$ per genotype). Mice were deeply anesthetized with isoflurane and transcardially perfused. Brains were post-fixed in paraformaldehyde (4%), cryopreserved in 30% sucrose, and 40- μ m coronal sections were cut on a cryostat (Leica, Germany). Free-floating sections were incubated at 4 °C for 48 h with anti-*c-Fos* antibody (Santa Cruz Biotechnology Inc., Santa Cruz, CA, USA). The primary antibody was detected using a Vectastain Elite ABC kit (Vector Laboratories, Burlingame, Ca, USA), and the diaminobenzidine reaction product was developed using a nickel-enhanced glucose oxidase method (Vector Laboratories, Burlingame, Ca, USA). The sections were mounted on Superfrost Plus slides (Fisher Scientific) and counterstained with Neutral Red. Cell counting was performed using Imaris software (Bitplane Scientific Solutions) on images captured under 40 \times magnification. Using a 10 \times 10 grid on which the specific region of interest was outlined, *Fos*-positive cells were counted within the hippocampus, somatosensory cortex (cortex), thalamus (paraventricular thalamic nucleus (PVT)), hypothalamus (paraventricular hypothalamic nucleus (PVN)), caudate nucleus (CN), lateral septal nucleus (LS), substantia nigra (STN), dorsal raphe (DR), locus coeruleus (LC), and nucleus accumbens (NA). The hippocampus was further divided into subregions: CA1, CA2–3, and the dentate gyrus (DG).

2.7. Histology

Two months after exposure to the A/PFE, 3 mutants and 3 WT littermates and an equal number of corresponding control mice were sacrificed for histological analysis. Brains were rapidly removed, frozen on dry ice, and 35- μ m sections were cut on a cryostat (Leica, Germany). Coronal sections, 400 μ m apart, from Bregma -0.46 mm to -3.38 mm, were examined. Sections were stained with 1% cresyl violet (CV, Sigma), and cell counts were performed using Imaris software (Bitplane Scientific Solutions) on images captured under 40 \times magnification. Using 10 \times 10 grids outlining the regions of interest, CV-positive cells were counted within the somatosensory cortex and the CA1, CA3, and dentate gyrus (DG) hippocampal regions.

2.8. Behavior analysis

2.8.1. Open field

The open field consisted of a 60 \times 60 cm² arena enclosed with opaque Plexiglas. The center zone was defined as a 30 \times 30 cm² area in the center of the chamber. Each mouse was placed along one side of the apparatus and allowed to explore for 10 min (13 male/genotype/treatment). Mice

were videotaped and scored with experimenters blind to genotype and treatment using the ANY-maze Video Tracking System (Stoelting Co.). Behaviors scored included time spent in the center zone, latency to enter the center zone, total distance traveled, average speed, and total time spent immobile.

2.8.2. Three chamber social interaction

Social recognition and memory were examined using a three-chambered apparatus. Each chamber measured 20 cm \times 40 cm \times 22 cm (h), and the partitions that separated each chamber had a 5 cm \times 5 cm square opening in the bottom center. A cylindrical wire cage, served as the inanimate object or the cage for housing the stranger mice. The test mouse (13 male/genotype/treatment) was first placed in the center chamber, with an empty wire cage in the left and the right chambers, and allowed to explore for 10 min. In the second 10-min session, an age- and gender-matched FVB/NJ mouse (stranger) was placed in one of the wire cages while the wire cage on the other side remained empty. The test mouse was again placed in the center chamber and allowed to explore. For the third 10-min session, a second age- and gender-matched FVB/NJ stranger mouse (novel mouse) was placed in the wire cage that previously served as the empty cage. Thus, the test mouse had a choice between a familiar mouse and a novel mouse. The test mouse was again placed in the center chamber and allowed to freely explore for 10 min. All three sessions were videotaped and the video was analyzed by an experimenter blind to genotype and treatment using the ANY-Maze Video Tracking System (Stoelting Co.). The times spent in each chamber and within 5 cm of each wire cage were measured.

2.8.3. Novel object recognition

The novel object test was used to evaluate recognition memory. Testing was conducted in the open field arena described above. The paradigm involved 4 days of testing. On day 1, each mouse (13 male/genotype/treatment) was placed in the empty arena and allowed to explore for 10 min. On days 2 and 3, each mouse was allowed to explore two identical objects (either a clear 11.5 \times 8.9 cm cube or a clear 10 cm diameter sphere) for 10 min, and the amount of time spent exploring each object was determined. To test for recognition memory, on Day 4, one of the objects was replaced with a novel object (cube replaced with sphere or vice versa) and the amount of time spent exploring each object was used to calculate a discrimination ratio (time exploring the novel object/(time exploring the novel object + time exploring the familiar object)). The objects were counterbalanced so that half of the mice of each genotype were either exposed to the cube or sphere on days 2 and 3. The mice were videotaped, and the videos analyzed by an experimenter blind to genotype and treatment using the ANY-Maze Video Tracking System (Stoelting Co.). Methodologies for Novel cage and Forced swim test are provided as Supplementary Data.

2.9. Slice preparation and recording

Slice recordings were performed on 4 experimental groups: WT controls, WT mice that had undergone the A/PFE, *RH/+* controls, and *RH/+* mice that had undergone the A/PFE. To prepare brain slices, 2.5–5-month-old mice were deeply anesthetized with halothane, rapidly decapitated, and their brains were removed. Horizontal hippocampal slices were cut 350 μ m thick with a vibratome (VT1200S; Leica Systems, Germany) in ice-cold sucrose-containing artificial cerebrospinal fluid (CSF) (in mM: 85 NaCl, 75 sucrose, 2.5 KCl, 25 glucose, 1.25 NaH₂PO₄, 4 MgCl₂, 0.5 CaCl₂, and 24 NaHCO₃). Slices were incubated in oxygenated normal ACSF (in mM: 126 NaCl, 2.5 KCl, 26 NaHCO₃, 2 CaCl₂, 2MgCl₂, 1.25 NaH₂PO₄, and 10 glucose) for 30 min to 1 h at 27 °C. All solutions used in preparation and recording were oxygenated by bubbling 95% O₂–5% CO₂.

Electrophysiological recordings were obtained using a MultiClamp 700B amplifier (Molecular Devices, Union City, CA) and digitized with a Digidata 1322A digitizer (Molecular Devices), and data were acquired

and analyzed with pClamp 10.2 software (Molecular Devices). Signals were sampled at 25 kHz and filtered at 10 kHz. The pipette solution contained the following (in mM): 126 K-gluconate, 4 KCl, 10 HEPES, 4 Mg-ATP, 0.3 Tris-GTP, and 10 Phospho-creatine, pH 7.2. The bath solution contained the following (in mM): 126 NaCl, 1.25 NaH₂PO₄, 2.5 KCl, 2 CaCl₂, 2 Mg Cl₂, 26 NaHCO₃, and 10 glucose, pH 7.3. Whole-cell recordings were obtained with access resistance < 30 MΩ, and cells were held at −70 mV for all experiments. Cells were visualized using infrared DIC illumination under 40× magnification. Hyperpolarizing current injections of −10 pA and −30 pA were used to calculate cellular impedance. All cell impedances were in the 300–350 MΩ range. Firing patterns were recorded in response to 2-second depolarizing current injections in 20-pA increments, starting at 10 pA, up to 190 pA. For epileptiform activity measurements, cells were held in voltage-clamp mode at −70 mV in normal (2.5 mM) K⁺ oxygenated ACSF to determine baseline bursting activity. Cells were then depolarized by perfusing high (8.5 mM) K⁺ ACSF for 10 min, during which epileptiform bursting activity was recorded, followed by a washout for 5 min. The events above a selected threshold between 8 and 16 pA in a 1-minute window were analyzed to determine amplitude and frequency. Events elicited in the presence of high K⁺ were compared to those in regular ACSF.

2.10. Statistical analysis

The Student *t*-test was used when comparing two sets of unrelated parametric data. Parametric data sets consisting of two or more variables were analyzed using a two-way analysis of variance (ANOVA) followed by a Tukey's pairwise comparison test. The Mann-Whitney Rank Sum test was used when comparing two sets of unrelated non-parametric data, and greater numbers of variables were compared using the Kruskal-Wallis test. In the novel object recognition test, which compared a specific response to the response expected by chance (50%), a one-tailed *t*-test was used. A one-way or 2-way ANOVA followed by Holm-Sidak's test for multiple comparisons was used to identify statistically significant differences in the firing rates of hippocampal neurons, intrinsic firing properties and excitatory activity of *RH* mutant mice and WT littermates. For ANOVA results that did not produce a significant interaction between the two factors, post hoc comparisons were still made. These analyses were continued due to the error rate (alpha, α) being still properly controlled with multiple post hoc comparisons even in the absence of a significant interaction (Hancock and Klockars, 1996; Ware et al., 2012). In these instances, both interaction and Tukey's Post Hoc values are listed. Dichotomous data were analyzed using the Fisher Exact test. All results were considered statistically significant if $p \leq 0.05$.

3. Results

3.1. *RH* mutants exhibit increased susceptibility to hyperthermia-induced seizures

We first examined FS susceptibility in *RH* mutants and WT littermates at 3 different ages: P14–15, P22–24, and P32–33. Each mouse was held at 37.5 °C for 30 min to determine baseline EEG activity. The temperature was then increased by 0.5 °C until a seizure was observed or 42.5 °C was reached. Simultaneous EEG analysis was conducted in order to determine whether behavioral seizures coincided with generalized spike discharges. Supplementary Fig. 1 shows representative EEG traces from *RH/+* and *RH/RH* mice during FS induction.

No seizures were observed in the WT mice at any age under these conditions. In contrast, seizures were observed in 75% (6/8) of *RH/+* mutants in the P14–15 age group, and in all of the P22–24 (8/8) and P32–33 (9/9) *RH/+* mutants (Fig. 1A). No differences were found in the average temperature at seizure induction between the different age groups of *RH/+* mice (Supplementary Table 1); however, average seizure duration, calculated by measuring the total length of the seizure presented on the EEG trace, was significantly longer in P14–15 *RH/+*

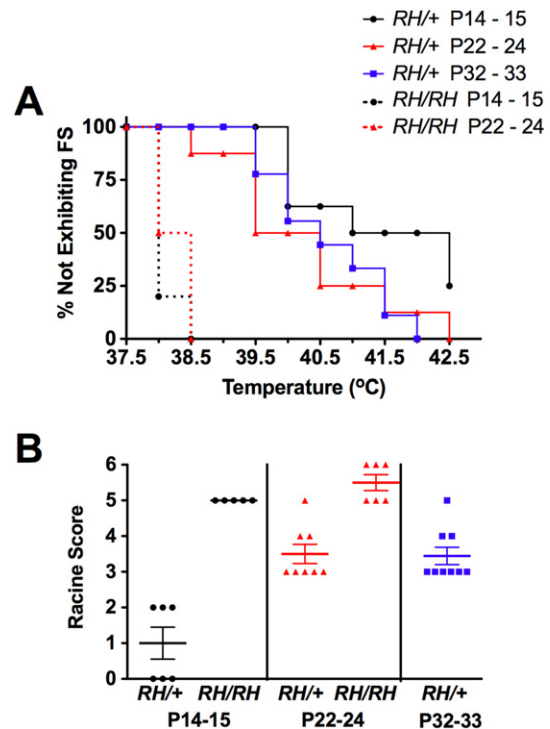


Fig. 1. *RH* mutants show greater susceptibility to hyperthermia-induced seizures. A. Susceptibility to acute hyperthermia-induced seizures was evaluated at 3 different ages: P14–15, P22–24, and P32–33. B. Seizure severity, based on a modified Racine scale, was determined.

mutants (Supplementary Table 1). EEG-detected seizure activity was associated with behavioral seizures in all P22–24 and P32–33 *RH/+*, but only in 50% (3/6) of the P14–15 *RH/+* mice (Fig. 2). There was no significant difference in the duration of EEG-detected seizures in mutants with or without accompanying behavioral components. Mice in the P22–24 and P32–33 age groups displayed behavioral seizures that scored higher on the Racine scale than in P14–15 *RH/+* mice (Fig. 1B, Supplementary Table 1). Specifically, P14–15 *RH/+* mice had seizures that were typically associated with staring (Average Racine score = 1.0 ± 0.4 , Fig. 1B, Supplementary Table 1), whereas the seizures observed in the P22–24 and P32–33 *RH/+* mice involved forelimb clonus and rearing and falling (Average Racine score: P22–24 = 3.5 ± 0.3 , P32–33 = 3.4 ± 0.2 , Fig. 1B, Supplementary Table 1).

Seizures were observed in all P14–15 (5/5) and P22–24 (6/6) *RH/RH* mice (Fig. 1A). There were no statistically significant differences in the average temperature at seizure onset, seizure duration, and seizure severity between P14–15 and P22–24 *RH/RH* mice (Supplementary Table 1). Because of the premature lethality of *RH/RH* mutants, it was not possible to examine older homozygous mutants.

We also compared the characteristics of the acutely induced seizures between *RH/RH* and *RH/+* mice. The seizures in the *RH/RH* mice were induced at lower average temperatures compared to similarly aged *RH/+* mice (P14–15: *RH/RH*, 38.1 ± 0.2 °C vs. *RH/+*, 41.3 ± 0.5 °C. P22–24: *RH/RH*, 38 ± 0.1 °C vs. *RH/+*, 40.4 ± 0.5 °C) and lasted longer (P14–15: *RH/RH*, 83 ± 6.7 s vs. *RH/+*, 37 ± 6.9 s. P22–24: *RH/RH*, 76 ± 7.7 s vs. *RH/+*, 13 ± 1.5 s) (Supplementary Table 1). Seizures in the *RH/RH* mutants, characterized by rearing and falling behaviors and progression to GTCS, were also more severe than those observed in *RH/+* mice (Fig. 1B, Supplementary Table 1).

3.2. Hyperthermia-induced seizures in *RH/+* mutants primarily activate neurons in the hippocampus

RH/+ mutants (P22, $n = 8$ (4 males and 4 females) were sacrificed 2 h after acute FS induction. WT littermates (P22, $n = 8$ (4 males and

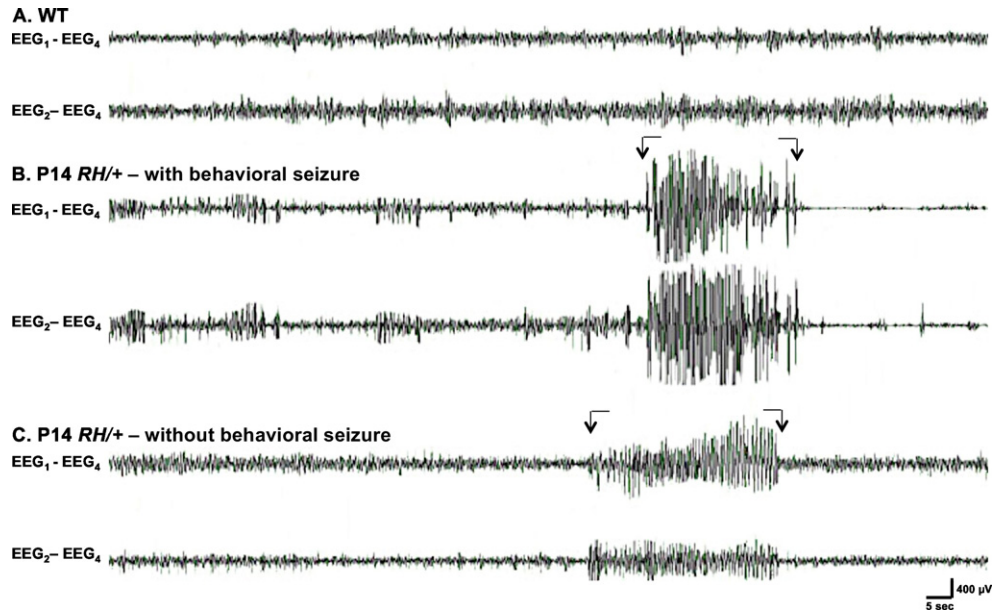


Fig. 2. EEG activity during acute FS induction in P14 mice. Representative EEG recordings during hyperthermia: (A) P14 WT mouse, (B) P14 *RH/+* mutant with behavioral seizure, and (C) P14 *RH/+* mutant without behavioral seizure. Arrows indicate seizure activity. Two cortical electrodes EEG₁ and EEG₂ were each referenced the fourth cortical electrode (EEG₄) to generate the EEG – REF montage: (e.g. EEG₁-EEG₄).

4 females) did not display seizure activity, but their core temperatures were raised to 42.5 °C followed by sacrifice 2 h later. *c-Fos* immunoreactivity was examined in the hippocampus (CA1, CA2, CA3, and DG), cortex, PVT, PVN, CN, LS, STN, DR, LC, and NA from both groups of mice. No statistically significant differences were observed between sexes; therefore, male and female data were combined. With the exception of DG, PVT, and LC the numbers of *c-Fos*-positive cells in corresponding brain regions were comparable between *RH/+* and WT mice (Fig. 3, Supplementary Table 2). *RH/+* FS mice showed significantly higher *c-Fos* immunoreactivity in the DG region of the hippocampus when compared to WT littermates, indicating this brain region is specifically activated during an acute FS (Fig. 3). *c-Fos* immunoreactivity was greater in the

PVT and the LC of the WT littermates that were subjected to the paradigm (Fig. 3, Supplementary Table 2), suggesting that activation of these brain regions was possibly due to exposure to the higher temperatures and/or the stress associated with the longer time spent in the cylinder.

3.3. Behavioral seizures produced during the 30-minute period of hyperthermia coincide with electrographic seizure activity

To model the effect of early-life, prolonged FSs, we designed the PFE paradigm in which mice were held at 41.5 °C for 30-minute. Behavioral seizures were observed in the P22–23 *RH/+* mutants but not the WT littermates during this period. To determine whether the observed behaviors reflected electrographic seizures, we first performed video/EEG recordings in a cohort of male mice ($n = 4\text{--}5/\text{genotype}$) during this period. The seizures that occurred consisted of generalized spike-discharges that were followed by postictal suppression of the background EEG. Epileptiform activity was accompanied by stereotypical behaviors that were scored based on a modified Racine scale that ranged from staring (score of 1) to a clonic seizure (score of 6). The average length of the seizures observed during the 30-minute temperature-holding period was longer than those generated by acute FS induction in the P22–23 mutants (PFE: 27 ± 3.5 s vs. Acute: 13 ± 1.5 s; $p = 0.02$).

3.4. More seizures occurred during the A/PFE paradigm compared to the PFE paradigm

The A/PFE and PFE paradigms differ in only one way: in the A/PFE paradigm, mice are exposed to an acute FS on day one prior to the 30-minute 41.5 °C period on day 2. To determine whether the acute FS component of the A/PFE paradigm affected seizure susceptibility on day 2, we compared the characteristics of the seizures that were generated during the 30-minute 41.5 °C holding period of both paradigms (Table 1). During the initial portion of each paradigm, the core body temperature of the mouse was increased by 0.5 °C every 2 min until it reached 41.5 °C. The average latency and temperature at which the first seizure occurred was noted for each paradigm; however, no statistically significant differences were observed. Next, we measured the total number of seizures experienced during each paradigm.

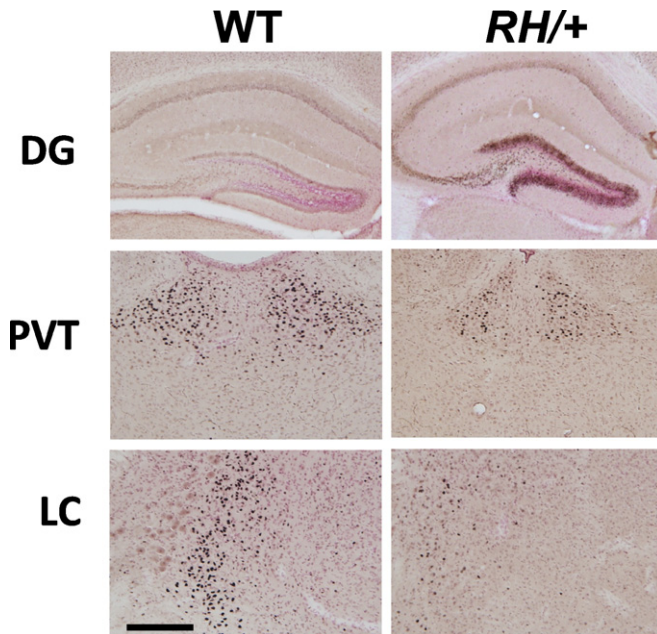


Fig. 3. Acute FS generation is associated with increased neuronal activity in the hippocampus. Representative *c-Fos* immunoreactivity in the dentate gyrus (DG), thalamus (paraventricular thalamic nucleus (PVT)), and locus coeruleus (LC) from P22 WT and *RH/+* mice 2 h post-acute seizure induction. 40 \times magnification, scale bar, 100 μ m.

Table 1

Comparison of seizure characteristics due to the PFE and A/PFE paradigms.

The average temperature of the first FS, average latency of the first FS, average seizure severity, and average total number of seizures experienced during each paradigm are shown. Average temperature, latency and total number of seizures were analyzed with the Student *t*-test. The Mann-Whitney test was used for seizure severity. A statistically significant difference was identified in the total number of seizures observed in the mice that were subjected to the PFE paradigm compared to the A/PFE paradigm. **p* < 0.05. Values are shown as mean ± SEM. 12 mice for each genotype and treatment were evaluated per paradigm.

	Average temperature at 1st seizure (°C)	Average latency to 1st seizure (s)	Average severity	Total number of seizures
PFE	41.1 ± 0.2	802 ± 58.0	2.6 ± 0.2	1.3 ± 0.2
A/PFE	40.8 ± 0.2	765 ± 44.7	2.9 ± 0.2	2.9 ± 0.7*

Approximately 2 times more seizures were observed in the group of mice that went through the A/PFE when compared to those subjected to the PFE (A/PFE: 2.9 ± 0.7 vs. PFE: 1.3 ± 0.2, *p* ≤ 0.05; Mann-Whitney test). However, the average severity of the seizures generated by both paradigms was comparable (Table 1).

3.5. Early-life FS events result in a further reduction of latencies to flurothyl-induced seizures in adulthood

Two separate cohorts of *RH/+* mutants and WT littermates (P22) were subjected to either the PFE or the A/PFE paradigm and then returned to normal housing conditions for a period of 2 months. Latencies to the flurothyl-induced seizure phenotypes (MJ, GTCS, and GTCS with HE) were then evaluated for each mouse. *RH/+* and WT littermates that were similarly handled but not subjected to elevated temperatures served as controls. Exposure to the PFE and A/PFE did not significantly alter latencies to any of the observed seizure stages in the WT mice (Fig. 4). As we previously reported, no difference was seen in the average latency to the MJ between control *RH/+* and control WT littermates (Fig. 4A) (Martin et al., 2010; Dutton et al., 2011). However, average latencies to the MJ were reduced by 18% and 29% in the mutants following the PFE and A/PFE paradigms, respectively, when compared to the control *RH/+* mice (*p* ≤ 0.001; 2-way ANOVA). Consistent with our previous observations, the average latency to the first GTCS was 13% lower in the control *RH/+* mutants compared to control WT littermates (*p* ≤ 0.05; 2-way ANOVA, Fig. 4B). Following the PFE, the average latency to the GTCS in *RH/+* mutants was reduced by 14% compared to the control *RH/+* mutants, but this difference was not statistically significant (*p* = 0.1; 2-way ANOVA); however, the latency to the GTCS in *RH/+* mutants was reduced by 33% compared to control *RH/+* mutant mice following the A/PFE (*p* < 0.001; 2-way ANOVA). No difference in the latency to GTCS with HE was observed in control *RH/+* mutants compared to control WT littermates (Fig. 4C); however, the latency to the GTCS with HE in *RH/+* mutants was reduced by 24% (*p* ≤ 0.01; 2-way ANOVA) and 45% (*p* ≤ 0.001; 2-way ANOVA) following the PFE and A/PFE, respectively, when compared to control *RH/+* mutants. These results demonstrate that complex early-life FS events increase susceptibility to flurothyl-induced seizures in adult *RH/+* mice and that the magnitude of the effect is influenced by the history of early-life FSs.

3.6. Early-life FS events increase the severity of spontaneous seizures in adult *RH/+* mice

To determine if complex early-life FSs can also lead to increased spontaneous seizure frequency and severity, we subjected *RH/+* mice and WT littermates (P22) to the A/PFE paradigm, and then performed longitudinal continuous video/EEG analysis when each mouse was 2–3 months old (120 h each mouse), 3–4 months old (24 h each mouse), 4–5 months old (24 h each mouse), and 7 months old (72 h each mouse). Similar video/EEG analysis was performed on age-matched control *RH/+* mice and WT littermates that were not subjected

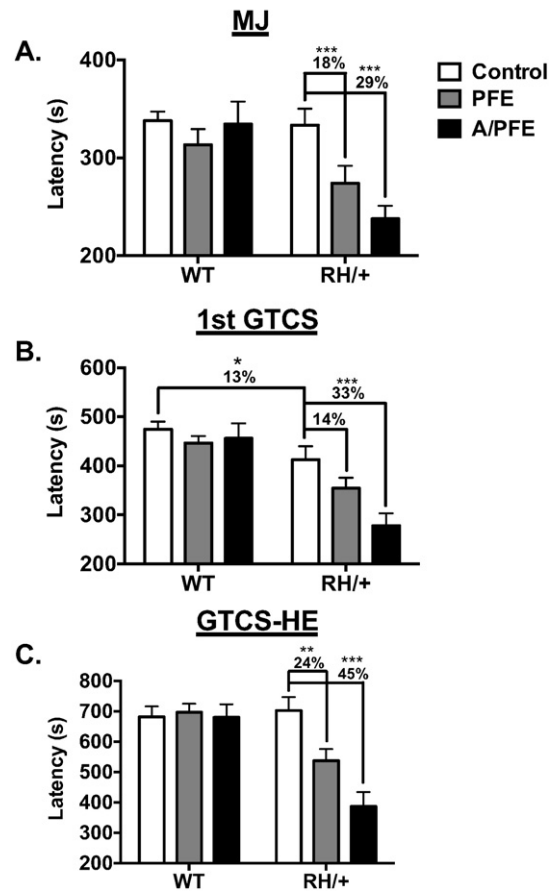


Fig. 4. Early-life FSs increase susceptibility to flurothyl-induced seizures in adult *RH/+* mutants. The latencies to the (A) myoclonic jerk (MJ), (B) the first generalized tonic clonic seizure (GTCS), and (C) the generalized tonic clonic seizure with hindlimb extension (GTCS-HE) were compared between WT and *RH/+* mice subjected to the PFE and A/PFE paradigms and control mice. **p* < 0.05, ***p* < 0.01, ****p* < 0.001. Data are shown as mean ± standard error of the mean (SEM).

to elevated heat. The characteristics of the seizures detected in each mouse are shown in Supplementary Table 3. A video of a *RH/+* mouse four months after A/PFE having a spontaneous seizure along with the corresponding EEG trace is provided in the Supplementary data.

As expected, spontaneous seizures were not observed in the control WT mice (Table 2). Consistent with the low frequency of seizures in *RH/+* mutants (Martin et al., 2010) only one control *RH/+* mouse (1/9) displayed spontaneous seizures during the total video/EEG recording period. This mouse exhibited 2 EEG-confirmed behavioral seizures with an average Racine score of 1.5 ± 0.5. The first seizure was characterized by staring behavior (Racine score = 1), and the second with sudden cessation of activity accompanied by head nodding and gradual resumption of activity (Racine score = 2). Both seizures were observed during the 3–4-month recording period. A total of 13 EEG-confirmed

Table 2

The A/PFE paradigm leads to increased seizure severity in adult *RH/+* mice.

Values represent the percentage of mice exhibiting spontaneous seizures and the corresponding average seizure severity. Statistical analysis of the percentage of mice exhibiting seizures was determined with the Fisher exact test and seizure severity was compared with the Kruskal-Wallis test. A statistically significant difference was observed in the severity of the seizures in *RH/+* mice that were subjected to the A/PFE paradigm. **p* < 0.05. Values are shown as mean ± SEM.

	Controls		A/PFE	
	WT (n = 8)	<i>RH/+</i> (n = 9)	WT (n = 9)	<i>RH/+</i> (n = 11)
% Exhibiting seizures	0% (0/8)	11% (1/9)	11% (1/9)	45% (5/11)
Average severity	N/A	1.5 ± 0.5	0.5 ± 0.2	2.8 ± 0.4*

seizures were detected during the 2–3- and 3–4-month recording periods in 5/11 (45%) *RH/+* mice that were subjected to the A/PFE paradigm. Specifically, seizures were observed in 4 *RH/+* mice during the 2–3-month recording period and in 2 mice during the 3–4-month period (Supplemental Table 3). The observed seizures were associated with a variety of behavioral phenotypes, including unilateral clonic movements, bilateral clonic movements, and staring behavior (average Racine score = 2.8 ± 0.4). In 1 WT mouse (1/9) subjected to the A/PFE paradigm, 1 and 11 electrographic seizures were detected during the 3–4- and 4–5-month recording periods, respectively. These seizures were either accompanied by staring and gradual resumption of activity (Racine score = 1) or lacked a behavioral component (Racine score = 0), (average Racine score = 0.5 ± 0.2), and were therefore considered less severe than those seen in the *RH/+* mice that were subjected to the A/PFE paradigm. No seizure activity was detected during EEG recordings performed at the 7-month time period for any of the mice. Overall, the average severities of the observed seizures, based on the Racine scores, were highest in *RH/+* mutants that were subjected to the A/PFE paradigm (Table 2). These results indicate that complex early-life FSs also increase the severity of spontaneous seizures in *RH/+* mutants during adulthood.

3.7. No evidence of neuronal loss in adult mice subjected to A/PFE

We compared WT and *RH/+* mice 2 months after the A/PFE paradigm to age-matched controls in order to determine whether neuronal loss may have contributed to the more severe adult seizure phenotypes. Using CV staining ($n = 3$ per group), we found no statistically significant difference in average cells counts within the cortex or hippocampus between the different groups (Supplementary Table 4).

3.8. Early-life FSs lead to hyperactivity, and impairments in social behavior and recognition memory in adult *RH/+* mice

We evaluated adult *RH/+* and WT mice that were subjected to the A/PFE paradigm and controls (CON) in the novel cage test, open field test, 3-chamber social interaction paradigm, forced-swim test, and novel object recognition test. We found that *RH/+* mice subjected to the A/PFE paradigm displayed hyperactivity in the open field paradigm as revealed by increased average speed (CON: WT; 9.5 ± 0.7 cm/s, *RH/+*; 10.2 ± 0.7 cm/s; A/PFE: WT; 9.7 ± 0.7 cm/s, *RH/+*; 13.5 ± 1.2 cm/s; Interaction: $F(1,44) = 3.7$, $p = 0.06$; Tukey's Post Hoc: $p < 0.05$) and greater distance traveled (CON: WT; 57 ± 4.2 m, *RH/+*; 61 ± 0.4 m; A/PFE: WT; 58 ± 4.1 m, *RH/+*; 81 ± 7.5 m; Interaction: $F(1,44) = 3.4$, $p =$

0.07 ; Tukey's Post Hoc: $p < 0.05$) (Fig. 5A and B). There was no difference in the amount of time spent in the center zone between WT and *RH/+* from either treatment groups (CON: WT; 41 ± 5.1 s, *RH/+*; 36 ± 2.8 s; A/PFE: WT; 44 ± 3.7 s, *RH/+*; 44 ± 7.0 s; Interaction: $F(1,44) = 0.3$, $p = 0.6$) suggesting normal anxiety levels.

The 3-chambered social interaction task was used to evaluate social behavior. While all groups of mice spent significantly more time investigating the container housing the stranger mouse versus the empty container, the difference was not statistically significant for the *RH/+* mutants that were subjected to the A/PFE (Interaction: $F(3,80) = 0.2$, $p = 0.9$; Fig. 5C) suggesting a modest deficit in sociability. More strikingly, A/PFE *RH/+* mice spent comparable amounts of time with the familiar and the novel mouse (Fig. 5D, Familiar: 29 ± 6.2 s; Novel: 42.7 ± 8.1 s), suggesting a deficit in social recognition and memory (Interaction: $F(3,80) = 1.0$, $p = 0.4$; Fig. 5D).

The novel object recognition test was used to assess learning and memory. A discrimination ratio for time spent exploring a novel versus familiar object was calculated for *RH/+* and WT mice subjected to the A/PFE and control conditions. This score reflects the mouse's innate preference for the novel object compared to a lack of preference (50% of time spent with each object). We found that WT and *RH/+* control mice and WT A/PFE mice were able to discriminate between the novel and familiar object as indicated by the significantly $>50\%$ of time spent exploring the novel object (WT CON: $69 \pm 3.3\%$, *RH/+* CON: $63 \pm 5.7\%$, WT A/PFE: $67 \pm 5.0\%$; $p < 0.05$), suggesting their ability to learn was normal. However, *RH/+* mice subjected to the A/PFE spent comparable amounts of time with the novel and familiar object ($47 \pm 5.4\%$; $p = 0.3$) suggesting a deficit in recognition memory (Fig. 5E).

There were no statistically significant differences in the amount of time spent digging or grooming in the novel cage paradigm between the WT and *RH/+* mice subjected to the A/PFE and controls (Supplementary Table 5), indicating normal exploratory behaviors. The 2-way ANOVA detected a main effect of genotype with rearing, indicating that the *RH/+* mice spent more time rearing compared to the WT mice, regardless of treatment ($p = 0.03$). No statistically significant differences were observed between any of the groups of mice in the forced swim test (Supplementary Table 5).

3.9. Early-life FS events lead to increased firing of pyramidal neurons in the CA3 region of adult mice

We compared the firing frequencies of CA3 pyramidal neurons from *RH/+* and WT mice after the A/PFE paradigm to age-matched controls at

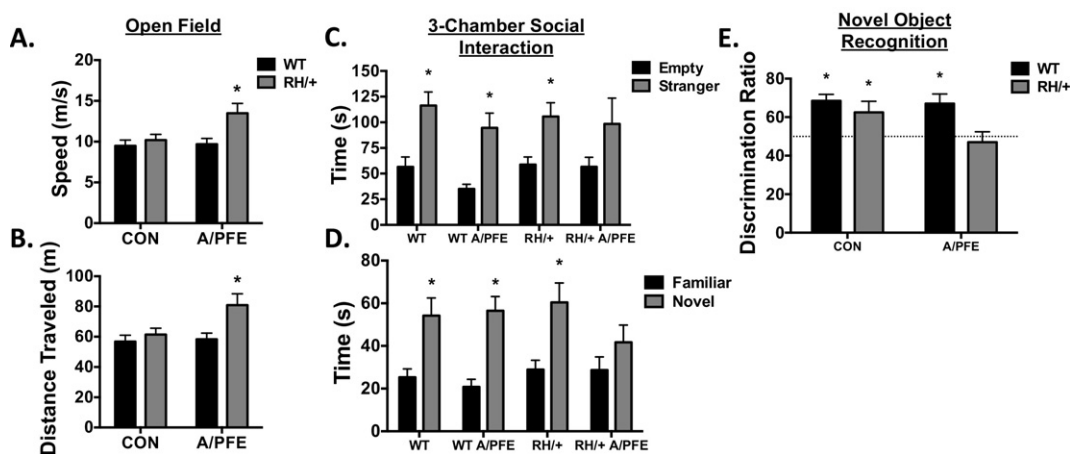


Fig. 5. A/PFE paradigm results in behavioral alterations in adult *RH/+* mice. (A–B) Open Field test: (A) *RH/+* mice exposed to the A/PFE move at faster speeds and (B) travel greater distances in an open field compared to WT mice subjected to the A/PFE and control WT and *RH/+* mice. (C–D) 3-Chamber Social Interaction test: (C) A/PFE *RH/+* mice spent more time with the stranger mouse when compared to the empty container, but the difference was not statistically significant. (D) A/PFE *RH/+* mice spent comparable amounts of time with the familiar and novel mouse. (E) Object Recognition Test: *RH/+* mice subjected to the A/PFE did not show a preference for the novel object, resulting in a discrimination index of $47 \pm 5.4\%$. $*p < 0.05$. Data are shown as mean \pm standard error of the mean (SEM).

current injections from 10 pA to 190 pA. The majority of pyramidal neurons we recorded from were regular accommodating or bursting (Graves et al., 2012) and this was the population used for analysis. Occasionally we identified neurons in the pyramidal layer that fired one AP instead of a train (1 in WT, 1 in *RH/+* and 2 in *RH/+ A/PFE*). These neurons were not included in the analysis because they either represented a different class of neuron or the access resistance changed during recording, indicating an unhealthy neuron. Pyramidal neurons had a resting membrane potential of ~ -70 mV and only neurons with an access resistance of less than or equal to 25 M Ω were used for analysis. There was no difference in cell impedance between the different groups, which were as follows: 333 ± 5 M Ω for WT, 336 ± 3 M Ω for *RH/+*, 337 ± 1 M Ω for WT A/PFE, 340 ± 3 M Ω for *RH/+ A/PFE*.

In pyramidal neurons from control WT mice, the number of action potentials (APs) continued to increase with increasing current injections (Fig. 6) to an average of 19 APs in 2 s at 190 pA. There was no significant difference between neurons from control WT and control *RH/+* mice, consistent with our previous results (Martin et al., 2010). A/PFE exposure did not affect the AP firing rates in pyramidal neurons from WT mice. However, *RH/+* mice that were subjected to A/PFE showed an increase in the firing of pyramidal neurons, and the higher rate of firing was significantly different compared to each of the other groups (Fig. 6). This increase in AP firing was likely due to the long-term effect of early-life FSs on neuronal excitability in *RH/+* mice that underwent A/PFE. This increase in pyramidal neuron AP firing would be predicted to increase network excitability.

Action potential firing thresholds were found to be significantly reduced in pyramidal neurons from *RH/+* and WT mice that had experienced A/PFE compared to control WT mice (Table 3). This observed reduction in firing thresholds would be predicted to lead to increased excitability. No significant differences were observed in half-width, maximum rise slope and after-hyperpolarization (Table 3).

Table 3

Intrinsic firing properties of CA3 pyramidal neurons.

AP threshold, peak, half-width, maximum rise slope, and AFP (after hyperpolarization) are shown as mean \pm SEM; * $p < 0.05$ compared to control WT; ** $p < 0.05$ compared to control WT and WT A/PFE; 1-way ANOVA followed by Holm-Sidak's test for multiple comparisons. n = number of cells.

	Control		A/PFE	
	WT ($n = 8$)	<i>RH/+</i> ($n = 6$)	WT ($n = 8$)	<i>RH/+</i> ($n = 5$)
AP threshold (mV)	-43 ± 1.6	-44 ± 2.2	$-52 \pm 2.2^*$	$-52 \pm 2.2^*$
AP peak (mV)	87 ± 2.1	$71 \pm 2.5^{**}$	86 ± 3.5	73 ± 5.5
AP half-width (ms)	2 ± 0.1	2 ± 0.3	2 ± 0.2	2 ± 0.2
AP max. rise slope (mV/ms)	144 ± 13.1	109 ± 14	137 ± 17.7	128 ± 24
AP AHP (mV)	-39 ± 1.7	-38 ± 6.5	-50 ± 7.3	-44 ± 3.6

3.10. Early-life FSs in *RH/+* mice lead to increased epileptiform activity during adulthood

To determine the effects of early-life FSs on network excitability, we compared bursting activity in CA3 pyramidal neurons from *RH/+* and WT after A/PFE to control mice in the presence of high (8.5 mM) extracellular K^+ . High K^+ has been shown to induce seizure-like bursting and large excitatory post-synaptic potentials in CA3 pyramidal neurons (Korn et al., 1987). The amplitude of high- K^+ induced excitatory activity in pyramidal neurons from control *RH/+* mice was not significantly different from that of control WT mice (Table 4). A/PFE caused a small but significant decrease in the amplitude of excitatory activity in neurons from WT mice. However, A/PFE resulted in a significant increase of approximately 1.5-fold in the excitatory amplitude in neurons from *RH/+* mice. There was also an increase of approximately 2.3-fold in the frequency of epileptiform activity recorded in high K^+ in *RH/+* after A/PFE

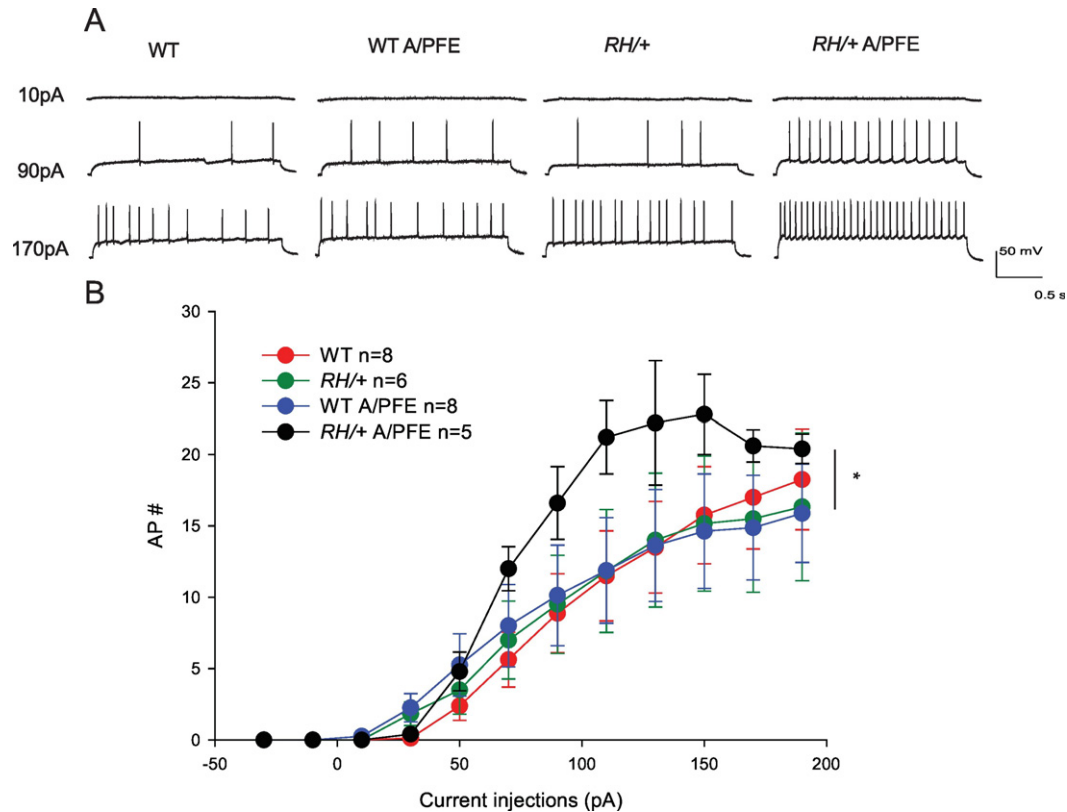


Fig. 6. A/PFE paradigm causes an increase in firing rates of mutant pyramidal CA3 neurons. (A) The firing patterns of pyramidal neurons from each of the 4 groups of mice are shown at current injections of 10 pA, 90 pA and 170 pA. (B) The number of APs fired in a 2-second period is plotted against the corresponding current injection. Data are shown as mean \pm SEM; n = number of cells. Statistical significance was determined by 2-way ANOVA, Holm-Sidak correction. *RH/+* mutants subjected to the A/PFE were significantly different ($p < 0.05$) from all other groups.

compared to control *RH/+* mutants (Table 4). There was no significant difference in frequency between control WT and A/PFE mice, but *RH/+* mice subjected to A/PFE fired action potentials at a frequency that was approximately 1.9-fold higher than WT mice subjected to A/PFE (Table 4). These increases in amplitude and frequency of epileptiform activity are consistent with increased network excitability (Table 4).

4. Discussion

Early-life FSs with a duration of ≤ 10 –15 min are not associated with the subsequent development of epilepsy in either prospective or retrospective studies (Verity et al., 1985; Berg and Shinnar, 1996). In contrast, 4–15% of patients that experience complex early-life FSs (seizures that are > 15 min in duration) are likely to develop epilepsy (Nelson and Ellenberg, 1976; Annegers et al., 1987). While this increased risk is low for the general population, it is possible that those with genetic predispositions such as *SCN1A* mutations are more affected by complex, early-life FSs. The long-term consequences of prolonged FSs (≥ 30 min) experienced in childhood are currently being examined in two longitudinal studies, FEBSTAT (Herrera et al., 2009; Nordli et al., 2012; Shinnar et al., 2012) and the London studies (Scott et al., 2002; Scott et al., 2003; Martinos et al., 2013). However information on the presence of genetic mutations in study participants is limited. Several studies have identified increased susceptibility to acutely induced hyperthermia seizures in rodent *Scn1a* models. Age-dependent susceptibility to hyperthermia-induced seizures were identified in the *Scn1a* mouse model of DS (Oakley et al., 2009) and these seizures were alleviated with the combined therapy of the anti-seizure drugs clonazepam and tiagabine (Oakley et al., 2013). The *Scn1a* GEFS+ rat model (Hiss) demonstrated increased susceptibility to acutely induced hyperthermia seizures (Mashimo et al., 2010), which resulted in activation of the limbic system (Ohno et al., 2011). However, prolonged or repetitive FSs induced between 3 and 5 weeks of age in this model did not result in seizures in the adults (Mashimo et al., 2010). Therefore, the role of complex FSs in long-term disease progression in these models is still unclear. Moreover, published clinical data from patients and families with *SCN1A* mutations are typically not detailed enough to allow research into this potential relationship. To fill this gap, we investigated the effect of early-life FSs on the development of epilepsy using a mouse line that expresses the human *SCN1A* GEFS+ mutation R1648H. We have previously demonstrated increased susceptibility to acute hyperthermia-induced seizures in this mouse model (Martin et al., 2010). To determine the long-term outcomes of early-life complex FSs, we subjected *RH/+* mice to a paradigm that models complex early-life FSs and evaluated their epileptic and behavioral phenotypes during adulthood. The main findings of this study are: (1) complex early-life FSs lead to increased seizure susceptibility, more severe spontaneous seizures, hyperactivity, and impairments in social behaviors and recognition memory during adulthood in *Scn1a* mutants; (2) the number of early-life FS events influences the severity of adult *Scn1a*-derived epilepsy; and (3) early-life FS exacerbates the effects of the R1648H mutation on neuron function.

Table 4

Amplitude and frequency of epileptiform activity. Amplitude and frequency of high K⁺ induced excitatory activity in pyramidal neurons are shown as mean \pm SEM; * $p < 0.05$ compared to control WT; ** $p < 0.05$ compared to control WT, control *RH/+* and WT A/PFE; 1-way ANOVA followed by Holm-Sidak's test for multiple comparisons. n = number of cells.

	Control		A/PFE	
	WT ($n = 9$)	<i>RH/+</i> ($n = 4$)	WT ($n = 4$)	<i>RH/+</i> ($n = 6$)
Amplitude (pA)	-23 ± 2.4	-19 ± 1.7	$-15 \pm 0.8^*$	$-29 \pm 0.7^{**}$
Frequency	35 ± 3.4	29 ± 11.0	35 ± 7.1	$67 \pm 3.9^{**}$

4.1. *RH* mutants are susceptible to hyperthermia-induced seizures

We previously reported that the P14–15 *RH/+* and *RH/RH* mice are susceptible to hyperthermia-induced seizures (Martin et al., 2010). Specifically, in our earlier report, average temperatures at FS induction in *RH/+* and *RH/RH* mutants occurred at 43.1 ± 0.3 °C and 40.4 ± 0.6 °C, respectively. These temperatures are higher than we saw in the current study for P14–15 mice (*RH/+*: 41.3 ± 0.5 ; *RH/RH*: 38.1 ± 0.2 ; Supplementary Table 1). We attribute this disparity, in part, to differences in the seizure induction methodology. In the previous study, body temperature was elevated rapidly using a stream of warm air. The current study used a thermostat-controlled heat lamp to provide a more gradual and controlled elevation of body temperature, thereby improving the sensitivity to measure seizure latency. In addition, our current study utilized mutant mice on a more advanced C57BL/6J genetic background. The C57BL/6J genetic background was previously shown to increase the severity of seizure phenotypes in *Scn1a* mutants (Yu et al., 2006; Sawyer et al., 2016).

Due to greater seizure susceptibility of the *RH/+* mutants, we were unable to identify conditions under which hyperthermia-induced seizures could be generated in both mutant and WT littermates during the prolonged FS paradigm without increasing the mortality of the mutants. The absence of seizures in the WT littermates during the 30-minute period of hyperthermia is therefore a potential caveat of our model. On the hand, the observation of greater sensitivity of the *RH/+* mutants to the effect of elevated temperatures is consistent with clinical observations.

In contrast to our results, studies that have examined susceptibility to hyperthermia-induced seizures in *Scn1a* knockout mouse models of Dravet syndrome have reported an inability to generate seizures in mice younger than 19 days old (Oakley et al., 2009; Rubinstein et al., 2015) despite demonstrated hippocampal hyperexcitability during this period (Liautard et al., 2013). This was surprising considering that mouse models of DS are generally considered to be more severely affected than GEFS+ mutants. The cause of this temporal difference in seizure susceptibility between the different lines is unclear. We speculate that it might reflect the effect of each type of mutation on channel function. It is possible that an alteration in the biophysical property of Na_v1.1 channels may have a greater effect on neuronal excitability when compared to a 50% reduction in protein levels during this period when the expression of the channel is still relatively low (Ogiwara et al., 2007).

4.2. The frequency of early-life FS events influences seizure severity during adulthood

To determine whether a history of early-life FS exposure could influence long-term seizure susceptibility, we subjected *RH/+* mutants and WT littermates to 2 different early-life FS paradigms and evaluated their susceptibility to flurothyl-induced seizures during adulthood. The PFE paradigm modeled a prolonged FS event, whereas in the A/PFE paradigm an acute FS preceded the prolonged event. While both paradigms resulted in further lowering of latencies to flurothyl-induced seizures in adult *RH/+* mutants, the magnitude of the reduction was greater in mutants that were subjected to the A/PFE paradigm. Neither paradigm altered thresholds in the WT littermates, highlighting the greater susceptibility of the mutants expressing the *Scn1a* mutation. We saw approximately 2 times more seizures during the 30-minute 41.5 °C holding period in the group of mice that were exposed to the A/PFE paradigm compared to the PFE paradigm (Table 1), indicating that seizure susceptibility during the 30-minute holding period was increased by prior exposure to an acute FS. The greater number of seizures during the A/PFE may have contributed to the more severe outcome associated with this paradigm, suggesting that the number of early-life FSs might influence epileptogenesis and clinical outcome. Based on our *c-Fos* data, the DG region of the hippocampus is significantly activated during acute FS induction.

4.3. Early-life FSs and long-term behavioral consequences

Previous studies reported conflicting effects of early-life FSs on cognitive function in rat models. Adult rats that were exposed to repetitive early-life FSs exhibited deficits in long-term memory that were associated with decreased expression of cAMP response element-binding protein (CREB) and translocation of CaMKII from the postsynaptic density to the cytosol (Chang et al., 2003; Xiong et al., 2014). In contrast, Lemmens et al. (2009) did not observe deficits in learning or locomotor activity in rat pups that were exposed to a single prolonged early-life FS and subsequently tested for behavioral impairments during adulthood. Similarly, while Notenboom et al. (2010) reported enhanced CA1 long-term potentiation (LTP) and reduced long-term depression (LTD) in adult rats that were subjected to a prolonged early-life FS as pups, no alterations in spatial learning or memory were observed.

In addition to seizures, patients with *SCN1A* mutations also manifest behavioral comorbidities such as attention-deficit disorder (ADHD)/hyperactivity, deficits in learning and memory, autistic behaviors and motor impairments (Wolff et al., 2006; Mahoney et al., 2009; Brunklaus et al., 2011; Genton et al., 2011; Li et al., 2011; Ragona, 2011; Tan et al., 2012). However, the association between recurrent and prolonged early-life FSs and the development of these clinically challenging phenotypes in patients with *SCN1A* mutations remains unclear and has never been experimentally investigated. Rodent models of *Scn1a* dysfunction recapitulate many of the cognitive and behavioral deficits reported in patients and therefore provide an opportunity to investigate this relationship (Han et al., 2012; Ito et al., 2013; Ohmori et al., 2014; Sawyer et al., 2016). While behavior was unaltered in *Scn1a* *RH/+* controls and WT littermates that were subjected to the A/PFE paradigm, early-life FS exposure in *Scn1a* *RH/+* mutants led to hyperactivity, deficits in social behaviors and impairments in recognition memory during adulthood, demonstrating the increased risk conferred by the *SCN1A* mutation. Surprisingly, although we previously observed hyperactivity and other behavioral abnormalities in adult *RH/+* mutants (Purcell et al., 2013) the behaviors of control *RH/+* mutants and control WT littermates were similar in the current study. A likely explanation for this difference is based on the genetic backgrounds of the mice that were used in these studies. The *RH/+* mutants that were used in the current study were backcrossed to C57BL/6J for 4 generations. In contrast, our previous behavioral studies were conducted on *RH/+* mutants that were backcrossed to C57BL/6J for 11–13 generations (Purcell et al., 2013; Sawyer et al., 2016). Yu et al. (2006) demonstrated that *Scn1a* knockout mice on an advanced (N10) C57BL6/J background display more severe phenotypes compared to those on a mixed 129/SvJ:C57BL6/J background. We also observed that *RH/+* mutants at the N12 generation had a higher mortality rate than at the N2 generation (Sawyer et al., 2016). Taken together, these results demonstrate that both genetic factors and environmental factors such as exposure to early life FSs are risk factors for the development of behavioral impairments in *Scn1a* mutant mice.

We previously showed that *Scn1a* is highly expressed in parvalbumin (PV) interneurons of the hippocampus and neocortex and deletion of *Scn1a* from this cell type results in epilepsy phenotypes (Dutton et al., 2013). The hippocampus is known to be an important brain structure for spatial learning (Foster and Knierim, 2012) and loss of GABAergic tone in the hippocampus due to reduction of PV interneurons results in hyperactivity and deficits in spatial memory (Reichel et al., 2014). In addition, the CA3 region of the hippocampus has been shown to be responsible for network oscillations that are critical for maintaining normal social behavior (Cellot et al., 2016). In our current study we found increased epileptiform activity in CA3 pyramidal neurons along with increased action potential firing in the A/PFE *Scn1a*^{*RH/+*} mice. We speculate that the enhanced CA3 network excitability might contribute to the observed behavioral alterations in these mice.

4.4. Hyperthermia and neuronal excitability

In our previous study of the *RH/+* mutants (Martin et al., 2010), we did not observe significant changes in pyramidal cell function even though there is evidence that Na_v1.1 is expressed in pyramidal neurons (Ogiwara et al., 2013). This was most likely because we recorded from young (P8–P10) mice. It was recently shown that differences in pyramidal neuron firing in *Scn1a*^{*+/-*} and WT mice do not become apparent until P21–P24 (Mistry et al., 2014). These authors also suggest that interneuron function is altered in pre-epileptic *Scn1a* mouse models of epilepsy, but pyramidal cell hyperexcitability might ultimately be responsible for seizures (Mistry et al., 2014). It has also been shown that alterations in interneuronal firing seen in *Scn1a*^{*+/-*} DS mice do not alter intrinsic network excitability in vivo (De Stasi et al., 2016). According to Hull and Isom (2016), there might be other factors such as pyramidal neuron hyperexcitability that alter the network dynamics during a seizure, and pyramidal neuron function has been shown to be altered in neurons derived from induced pluripotent stem cells from Dravet patients (Liu et al., 2013). For these reasons, we investigated the firing properties of pyramidal neurons in the current study, and we found increased excitability in CA3 pyramidal neurons of mutant mice that had undergone A/PFE.

We recorded from the CA3 region rather than the DG despite the fact that we observed c-fos staining in the DG for a number of reasons. First, in *Scn1b* null mutants, epileptiform activity was observed in the CA3 of the hippocampus but not in the DG, despite noticeable c-fos staining in the DG of those mice (Brackenburg et al., 2013). Second, CA3 neurons receive direct input from granule cells of the DG and ‘backproject’ onto the DG, making CA3 the ‘gateway to the hippocampus’ (Scharfman, 2007). High levels of spontaneous activity in CA3 pyramidal cells makes them vulnerable to neuronal depolarization upon DG mossy fiber stimulation. In kainate-induced epilepsy, Yu et al. showed that silencing CA3 pyramidal cells is sufficient to attenuate seizures (Yu et al., 2016). Finally, FSs are known to affect neurons in the CA3 region of the hippocampus (Kim and Connors, 2012).

In our previous study (Martin et al., 2010), we observed differences in interneuron firing properties resulting from the R1648H mutation. However, those results were obtained from dissociated cortical interneurons (bipolar neurons) that were identified by shape and most likely represent a sub-population of basket cells (Markram et al., 2004). Quantitative analysis of the properties of those interneurons in hippocampal slices would require prior labeling of interneuron populations (Monyer and Markram, 2004), which was beyond the scope of the current study.

To determine the net effect of individual cell firing on network properties, we measured spontaneous excitatory activity in hippocampal slices. Based on the increased amplitudes and frequency of epileptiform activity in *RH/+* mice that were subjected to the A/PFE paradigm, it appears that the overall effect of early-life FSs is to increase excitability in the CA3, with a more pronounced effect in *RH/+* mice.

The effect of hyperthermia on neuronal excitability has previously been investigated. Increased excitability in the seizure-prone CA3 region of the hippocampus was observed when immature hippocampal neurons were examined at 41 °C in slice preparations (Kim and Connors, 2012). Using whole-cell patch clamp, similar alterations were seen in cultured rat cortical neurons subjected to hyperthermia (Wang et al., 2011). Increased inhibitory pre-synaptic terminals were identified in CA3 neurons of P35 rats that were exposed to a prolonged FS paradigm at P8 (Feng et al., 2015). Our data showing decreased AP threshold in WT and *RH/+* neurons following A/PFE are consistent with these prior results. In addition, there are reports that acute hyperthermia decreases GABA_A receptor-mediated synaptic transmission onto CA1 pyramidal neurons (Qu et al., 2007; Qu and Leung, 2008; Qu and Leung, 2009), pointing to reduced network inhibition as a consequence of increased brain temperatures. Our data showing increased eEPSC amplitudes and frequency following A/PFE support the hypothesis that early-life FSs result in a long-term decrease in network inhibition.

4.5. Interventions to ameliorate the effects of early-life FSs

Our current study highlights the potential impact of complex early-life FSs on adult epilepsy in patients with *SCN1A* mutations. Previous data from *Scn1a* mutant mice identified reduced excitability of GABAergic interneurons as the main biophysical impairment, suggesting that the enhancement of GABA signaling might increase FS resistance. Accordingly, Cao et al. (2012) showed that the anticonvulsant stiripentol increases thresholds to hyperthermia-induced seizures in heterozygous *Scn1a* knockout mice. This drug enhances GABA_A receptor-mediated transmission in the hippocampus of immature animals due to its ability to increase the frequency and lengthen the decay time constant of miniature inhibitory postsynaptic currents (mIPSCs) (Quilichini et al., 2006). Similarly, the benzodiazepine clonazepam (a positive allosteric modulator of GABA_A receptors) and tiagabine (a presynaptic GABA_A receptor inhibitor) are also effective at preventing hyperthermia-induced seizures (Oakley et al., 2013). Further studies to determine whether GABA enhancement following the A/PFE paradigm could ameliorate the long-term effects on adult seizure phenotypes are warranted.

The inflammatory system is known to contribute to the generation of FSs via microglia activation and subsequent release of various cytokines, such as IL-1 β . Experimentally, IL-1 β receptor knockout mice (ILR1) display increased latencies to hyperthermia-induced seizures (Dube et al., 2005), and an exogenous IL-R antagonist inhibits FSs (Heida and Pittman, 2005). Increased levels of IL-1 β are also seen at the onset of experimentally induced FSs (Heida and Pittman, 2005) and in children following FSs (Haspolat et al., 2002). Drugs that target microglial activation, such as minocycline, may therefore reduce the long-term impact of early-life FSs. Experimentally, minocycline was shown to attenuate microglia activation and block the long-term effects of prolonged kainic acid-induced early-life seizures (Abraham et al., 2012), and reduce the after-discharge duration induced by amygdala kindling in rats (Beheshti Nasr et al., 2013). A recent study by Jongbloets et al. (2015) identified increased expression of proinflammatory genes 1 h after exposure to a prolonged FS paradigm in P10 C57BL/6 mice. Based on this finding, we speculate that early intervention with anti-inflammatory drugs may alter disease progression.

5. Conclusions

This study demonstrated that early-life prolonged FSs have a profound long-term impact on neuronal function and adult seizure phenotypes in a mouse model of human *SCN1A* dysfunction. These findings highlight the clinical importance of preventing FSs in this patient population and hold out the promise of improving disease outcomes through effective early pharmacological intervention.

Funding

This research was supported by grants from NIH to AE (NS072221), ALG (NS048336), AE/ALG (NS065187) and an NIH/NIGMS IRACDA grant to SD (K12 GM000680).

Acknowledgements

We thank Drs. Wen-Pin Chen and Christine McLaren for assistance with the statistical analysis using Generalized Estimated Equations. We also thank Cheryl Strauss for editorial assistance.

Appendix A. Supplementary data

Supplementary data to this article can be found online at <http://dx.doi.org/10.1016/j.expneurol.2017.03.026>.

References

- Abraham, J., Fox, P.D., Condello, C., Bartolini, A., Koh, S., 2012. Minocycline attenuates microglia activation and blocks the long-term epileptogenic effects of early-life seizures. *Neurobiol. Dis.* 46 (2), 425–430.
- Annegers, J.F., Hauser, W.A., Shirts, S.B., Kurland, L.T., 1987. Factors prognostic of unprovoked seizures after febrile convulsions. *N. Engl. J. Med.* 316 (9), 493–498.
- Baram, T.Z., Gerth, A., Schultz, L., 1997. Febrile seizures: an appropriate-aged model suitable for long-term studies. *Brain Res. Dev. Brain Res.* 98 (2), 265–270.
- Beheshti Nasr, S.M., Moghimi, A., Mohammad-Zadeh, M., Shamsizadeh, A., Noorbakhsh, S.M., 2013. The effect of minocycline on seizures induced by amygdala kindling in rats. *Seizure* 22 (8), 670–674.
- Bender, R.A., Dube, C., Gonzalez-Vega, R., Mina, E.W., Baram, T.Z., 2003. Mossy fiber plasticity and enhanced hippocampal excitability, without hippocampal cell loss or altered neurogenesis, in an animal model of prolonged febrile seizures. *Hippocampus* 13 (3), 399–412.
- Berg, A.T., Shinnar, S., 1996. Unprovoked seizures in children with febrile seizures: short-term outcome. *Neurology* 47 (2), 562–568.
- Brackenbury, W.J., Yuan, Y., O'Malley, H.A., Parent, J.M., Isom, L.L., 2013. Abnormal neuronal patterning occurs during early postnatal brain development of *Scn1b*-null mice and precedes hyperexcitability. *Proc. Natl. Acad. Sci. U. S. A.* 110 (3), 1089–1094.
- Brewster, A., Bender, R.A., Chen, Y., Dube, C., Eghbal-Ahmadi, M., Baram, T.Z., 2002. Developmental febrile seizures modulate hippocampal gene expression of hyperpolarization-activated channels in an isoform- and cell-specific manner. *J. Neurosci.* 22 (11), 4591–4599.
- Brewster, A.L., Bernard, J.A., Gall, C.M., Baram, T.Z., 2005. Formation of heteromeric hyperpolarization-activated cyclic nucleotide-gated (HCN) channels in the hippocampus is regulated by developmental seizures. *Neurobiol. Dis.* 19 (1–2), 200–207.
- Brunklaus, A., Dorris, L., Zuberi, S.M., 2011. Comorbidities and predictors of health-related quality of life in Dravet syndrome. *Epilepsia* 52 (8), 1476–1482.
- Cao, D., Ohtani, H., Ogiwara, I., Ohtani, S., Takahashi, Y., Yamakawa, K., Inoue, Y., 2012. Efficacy of stiripentol in hyperthermia-induced seizures in a mouse model of Dravet syndrome. *Epilepsia* 53 (7), 1140–1145.
- Cellot, G., Maggi, L., Di Castro, M.A., Catalano, M., Migliore, R., Migliore, M., Scattoni, M.L., Calamandrei, G., Cherubini, E., 2016. Premature changes in neuronal excitability account for hippocampal network impairment and autistic-like behavior in neonatal BTBR T+tf/J mice. *Sci. Rep.* 6, 31696.
- Cendes, F., Andermann, F., Dubeau, F., Gloor, P., Evans, A., Jones-Gotman, M., Olivier, A., Andermann, E., Robitaille, Y., Lopes-Cendes, I., et al., 1993. Early childhood prolonged febrile convulsions, atrophy and sclerosis of mesial structures, and temporal lobe epilepsy: an MRI volumetric study. *Neurology* 43 (6), 1083–1087.
- Chang, Y.C., Huang, A.M., Kuo, Y.M., Wang, S.T., Chang, Y.Y., Huang, C.C., 2003. Febrile seizures impair memory and cAMP response-element binding protein activation. *Ann. Neurol.* 54 (6), 706–718.
- Chen, K., Baram, T.Z., Soltesz, I., 1999. Febrile seizures in the developing brain result in persistent modification of neuronal excitability in limbic circuits. *Nat. Med.* 5 (8), 888–894.
- Chen, K., Aradi, I., Thon, N., Eghbal-Ahmadi, M., Baram, T.Z., Soltesz, I., 2001. Persistently modified h-channels after complex febrile seizures convert the seizure-induced enhancement of inhibition to hyperexcitability. *Nat. Med.* 7 (3), 331–337.
- De Stasi, A.M., Farisello, P., Marcon, I., Cavallari, S., Forli, A., Vecchia, D., Losi, G., Mantegazza, M., Panzeri, S., Carmignoto, G., Bacci, A., Fellin, T., 2016. Unaltered network activity and interneuronal firing during spontaneous cortical dynamics in vivo in a mouse model of severe myoclonic epilepsy of infancy. *Cereb. Cortex* 26 (4), 1778–1794.
- Dube, C., Brunson, K.L., Eghbal-Ahmadi, M., Gonzalez-Vega, R., Baram, T.Z., 2005. Endogenous neuropeptide Y prevents recurrence of experimental febrile seizures by increasing seizure threshold. *J. Mol. Neurosci.* 25 (3), 275–284.
- Dube, C., Richichi, C., Bender, R.A., Chung, G., Litt, B., Baram, T.Z., 2006. Temporal lobe epilepsy after experimental prolonged febrile seizures: prospective analysis. *Brain* 129 (Pt 4), 911–922.
- Dutton, S.B., Sawyer, N.T., Kalume, F., Jumbo-Lucioni, P., Borges, K., Catterall, W.A., Escayg, A., 2011. Protective effect of the ketogenic diet in *Scn1a* mutant mice. *Epilepsia* 52 (11), 2050–2056.
- Dutton, S.B., Makinson, C.D., Papale, L.A., Shankar, A., Balakrishnan, B., Nakazawa, K., Escayg, A., 2013. Preferential inactivation of *Scn1a* in parvalbumin interneurons increases seizure susceptibility. *Neurobiol. Dis.* 49, 211–220.
- Falconer, M.A., Serafetinides, E.A., Corsellis, J.A., 1964. Etiology and pathogenesis of temporal lobe epilepsy. *Arch. Neurol.* 10, 233–248.
- Feng, B., Chen, Z., 2016. Generation of febrile seizures and subsequent epileptogenesis. *Neurosci. Bull.* 32 (5), 481–492.
- Feng, B., Tang, Y.S., Chen, B., Xu, Z.H., Wang, Y., Wu, D.C., Zhao, H.W., Zhang, S.H., Chen, Z., 2015. Early hypoactivity of hippocampal rhythms during epileptogenesis after prolonged febrile seizures in freely-moving rats. *Neurosci. Bull.* 31 (3), 297–306.
- Foster, D.J., Knierim, J.J., 2012. Sequence learning and the role of the hippocampus in rodent navigation. *Curr. Opin. Neurobiol.* 22 (2), 294–300.
- French, J.A., Williamson, P.D., Thadani, V.M., Darcey, T.M., Mattson, R.H., Spencer, S.S., Spencer, D.D., 1993. Characteristics of medial temporal lobe epilepsy: I. Results of history and physical examination. *Ann. Neurol.* 34 (6), 774–780.
- Genton, P., Velizarova, R., Dravet, C., 2011. Dravet syndrome: the long-term outcome. *Epilepsia* 52 (Suppl. 2), 44–49.
- Gonzalez Ramirez, M., Orozco Suarez, S., Salgado Ceballos, H., Feria Velasco, A., Rocha, L., 2007. Hyperthermia-induced seizures modify the GABA(A) and benzodiazepine receptor binding in immature rat brain. *Cell. Mol. Neurobiol.* 27 (2), 211–227.

- Graves, A.R., Moore, S.J., Bloss, E.B., Mensh, B.D., Kath, W.L., Spruston, N., 2012. Hippocampal pyramidal neurons comprise two distinct cell types that are countermodulated by metabotropic receptors. *Neuron* 76 (4), 776–789.
- Han, Y., Qin, J., Bu, D.F., Chang, X.Z., Yang, Z.X., 2006. Successive alterations of hippocampal gamma-aminobutyric acid B receptor subunits in a rat model of febrile seizure. *Life Sci.* 78 (25), 2944–2952.
- Han, S., Tai, C., Westenbroek, R.E., Yu, F.H., Cheah, C.S., Potter, G.B., Rubenstein, J.L., Scheuer, T., de la Iglesia, H.O., Catterall, W.A., 2012. Autistic-like behaviour in *Scn1a*^{+/-} mice and rescue by enhanced GABA-mediated neurotransmission. *Nature* 489 (7416), 385–390.
- Hancock, G.R., Klockars, A.J., 1996. The quest for alpha: developments in multiple comparison procedures in the quarter century since Games (1971). *Rev. Educ. Res.* 66 (3), 296–306.
- Haspolat, S., Mihci, E., Coskun, M., Gumuslu, S., Ozben, T., Yegin, O., 2002. Interleukin-1beta, tumor necrosis factor-alpha, and nitrite levels in febrile seizures. *J. Child Neurol.* 17 (10), 749–751.
- Heida, J.G., Pittman, Q.J., 2005. Causal links between brain cytokines and experimental febrile convulsions in the rat. *Epilepsia* 46 (12), 1906–1913.
- Herrera, E.A., Alvarez, S.Y., Cobos, O., Villeda, T., 2009. Phenomenology of prolonged febrile seizures: results of the FEBSTAT study. *Neurology* 72 (17), 1533 (author reply 1533–1534).
- Hull, J.M., Isom, L.L., 2016. Expecting the unexpected: lack of in vivo network defects in an *Scn1a* model of Dravet syndrome. *Epilepsy Curr* 16 (6), 408–410.
- Ito, S., Ogiwara, I., Yamada, K., Miyamoto, H., Hensch, T.K., Osawa, M., Yamakawa, K., 2013. Mouse with *Nav1.1* haploinsufficiency, a model for Dravet syndrome, exhibits lowered sociability and learning impairment. *Neurobiol. Dis.* 49, 29–40.
- Jongbloets, B.C., van Gassen, K.L., Kan, A.A., Olde Engberink, A.H., de Wit, M., Wolterink-Donseelaar, I.G., Groot Koerkamp, M.J., van Nieuwenhuizen, O., Holstege, F.C., de Graan, P.N., 2015. Expression profiling after prolonged experimental febrile seizures in mice suggests structural remodeling in the hippocampus. *PLoS One* 10 (12), e0145247.
- Kim, J.A., Connors, B.W., 2012. High temperatures alter physiological properties of pyramidal cells and inhibitory interneurons in hippocampus. *Front. Cell. Neurosci.* 6, 27.
- Korn, S.J., Giachino, J.L., Chamberlin, N.L., Dingledine, R., 1987. Epileptiform burst activity induced by potassium in the hippocampus and its regulation by GABA-mediated inhibition. *J. Neurophysiol.* 57 (1), 325–340.
- Lemmens, E.M., Aendekerck, B., Schijns, O.E., Blokland, A., Beuls, E.A., Hoogland, G., 2009. Long-term behavioral outcome after early-life hyperthermia-induced seizures. *Epilepsy Behav.* 14 (2), 309–315.
- Li, B.M., Liu, X.R., Yi, Y.H., Deng, Y.H., Su, T., Zou, X., Liao, W.P., 2011. Autism in Dravet syndrome: prevalence, features, and relationship to the clinical characteristics of epilepsy and mental retardation. *Epilepsy Behav.* 21 (3), 291–295.
- Liautard, C., Scalmani, P., Carriero, G., de Curtis, M., Franceschetti, S., Mantegazza, M., 2013. Hippocampal hyperexcitability and specific epileptiform activity in a mouse model of Dravet syndrome. *Epilepsia* 54 (7), 1251–1261.
- Liu, Y., Lopez-Santiago, L.F., Yuan, Y., Jones, J.M., Zhang, H., O'Malley, H.A., Patino, G.A., O'Brien, J.E., Rusconi, R., Gupta, A., Thompson, R.C., Natowicz, M.R., Meisler, M.H., Isom, L.L., Parent, J.M., 2013. Dravet syndrome patient-derived neurons suggest a novel epilepsy mechanism. *Ann. Neurol.* 74 (1), 128–139.
- Mahoney, K., Moore, S.J., Buckley, D., Alam, M., Parfrey, P., Penney, S., Merner, N., Hodgkinson, K., Young, T.L., 2009. Variable neurologic phenotype in a GEFS+ family with a novel mutation in *SCN1A*. *Seizure* 18 (7), 492–497.
- Markram, H., Toledo-Rodriguez, M., Wang, Y., Gupta, A., Silberberg, G., Wu, C., 2004. Interneurons of the neocortical inhibitory system. *Nat. Rev. Neurosci.* 5 (10), 793–807.
- Martin, M.S., Dutt, K., Papale, L.A., Dube, C.M., Dutton, S.B., de Haan, G., Shankar, A., Tufik, S., Meisler, M.H., Baram, T.Z., Goldin, A.L., Escayg, A., 2010. Altered function of the *SCN1A* voltage-gated sodium channel leads to gamma-aminobutyric acid-ergic (GABAergic) interneuron abnormalities. *J. Biol. Chem.* 285 (13), 9823–9834.
- Martinos, M.M., Yoong, M., Patil, S., Chong, W.K., Mardari, R., Chin, R.F., Neville, B.G., de Haan, M., Scott, R.C., 2013. Early developmental outcomes in children following convulsive status epilepticus: a longitudinal study. *Epilepsia* 54 (6), 1012–1019.
- Mashimo, T., Ohmori, I., Ouchida, M., Ohno, Y., Tsurumi, T., Miki, T., Wakamori, M., Ishihara, S., Yoshida, T., Takizawa, A., Kato, M., Hirabayashi, M., Sasa, M., Mori, Y., Serikawa, T., 2010. A missense mutation of the gene encoding voltage-dependent sodium channel (*Nav1.1*) confers susceptibility to febrile seizures in rats. *J. Neurosci.* 30 (16), 5744–5753.
- Matsuo, M., Sasaki, K., Ichimaru, T., Nakazato, S., Hamasaki, Y., 2006. Increased IL-1beta production from dsRNA-stimulated leukocytes in febrile seizures. *Pediatr. Neurol.* 35 (2), 102–106.
- Mistry, A.M., Thompson, C.H., Miller, A.R., Vanoye, C.G., George Jr., A.L., Kearney, J.A., 2014. Strain- and age-dependent hippocampal neuron sodium currents correlate with epilepsy severity in Dravet syndrome mice. *Neurobiol. Dis.* 65, 1–11.
- Monyer, H., Markram, H., 2004. *Interneuron diversity series: molecular and genetic tools to study GABAergic interneuron diversity and function*. *Trends Neurosci.* 27, 90–97.
- Mullen, S.A., Scheffer, I.E., 2009. Translational research in epilepsy genetics: sodium channels in man to interneuronopathy in mouse. *Arch. Neurol.* 66 (1), 21–26.
- Nelson, K.B., Ellenberg, J.H., 1976. Predictors of epilepsy in children who have experienced febrile seizures. *N. Engl. J. Med.* 295 (19), 1029–1033.
- Nordli Jr., D.R., Moshe, S.L., Shinnar, S., Hesdorffer, D.C., Sogawa, Y., Pellock, J.M., Lewis, D.V., Frank, L.M., Shinnar, R.C., Sun, S., 2012. Acute EEG findings in children with febrile status epilepticus: results of the FEBSTAT study. *Neurology* 79 (22), 2180–2186.
- Notenboom, R.G., Ramakers, G.M., Kamal, A., Spruijt, B.M., de Graan, P.N., 2010. Long-lasting modulation of synaptic plasticity in rat hippocampus after early-life complex febrile seizures. *Eur. J. Neurosci.* 32 (5), 749–758.
- Oakley, J.C., Kalume, F., Yu, F.H., Scheuer, T., Catterall, W.A., 2009. Temperature- and age-dependent seizures in a mouse model of severe myoclonic epilepsy in infancy. *Proc. Natl. Acad. Sci. U. S. A.* 106 (10), 3994–3999.
- Oakley, J.C., Cho, A.R., Cheah, C.S., Scheuer, T., Catterall, W.A., 2013. Synergistic GABA-enhancing therapy against seizures in a mouse model of Dravet syndrome. *J. Pharmacol. Exp. Ther.* 345 (2), 215–224.
- Ogiwara, I., Miyamoto, H., Morita, N., Atapour, N., Mazaki, E., Inoue, I., Takeuchi, T., Itohara, S., Yanagawa, Y., Obata, K., Furuichi, T., Hensch, T.K., Yamakawa, K., 2007. *Na(v)1.1* localizes to axons of parvalbumin-positive inhibitory interneurons: a circuit basis for epileptic seizures in mice carrying an *Scn1a* gene mutation. *J. Neurosci.* 27 (22), 5903–5914.
- Ogiwara, I., Iwasato, T., Miyamoto, H., Iwata, R., Yamagata, T., Mazaki, E., Yanagawa, Y., Tamamaki, N., Hensch, T.K., Itohara, S., Yamakawa, K., 2013. *Nav1.1* haploinsufficiency in excitatory neurons ameliorates seizure-associated sudden death in a mouse model of Dravet syndrome. *Hum. Mol. Genet.* 22 (23), 4784–4804.
- Ohmori, I., Kawakami, N., Liu, S., Wang, H., Miyazaki, I., Asanuma, M., Michiue, H., Matsui, H., Mashimo, T., Ouchida, M., 2014. Methylphenidate improves learning impairments and hyperthermia-induced seizures caused by an *Scn1a* mutation. *Epilepsia* 55 (10), 1558–1567.
- Ohno, Y., Ishihara, S., Mashimo, T., Sofue, N., Shimizu, S., Imaoku, T., Tsurumi, T., Sasa, M., Serikawa, T., 2011. *Scn1a* missense mutation causes limbic hyperexcitability and vulnerability to experimental febrile seizures. *Neurobiol. Dis.* 41 (2), 261–269.
- Purcell, R.H., Papale, L.A., Makinson, C.D., Sawyer, N.T., Schroeder, J.P., Escayg, A., Weinschenker, D., 2013. Effects of an epilepsy-causing mutation in the *SCN1A* sodium channel gene on cocaine-induced seizure susceptibility in mice. *Psychopharmacology* 228 (2), 263–270.
- Qu, L., Leung, L.S., 2008. Mechanisms of hyperthermia-induced depression of GABAergic synaptic transmission in the immature rat hippocampus. *J. Neurochem.* 106 (5), 2158–2169.
- Qu, L., Leung, L.S., 2009. Effects of temperature elevation on neuronal inhibition in hippocampal neurons of immature and mature rats. *J. Neurosci. Res.* 87 (12), 2773–2785.
- Qu, L., Liu, X., Wu, C., Leung, L.S., 2007. Hyperthermia decreases GABAergic synaptic transmission in hippocampal neurons of immature rats. *Neurobiol. Dis.* 27 (3), 320–327.
- Quilichini, P.P., Chiron, C., Ben-Ari, Y., Gozlan, H., 2006. Stiripentol, a putative antiepileptic drug, enhances the duration of opening of GABA-A receptor channels. *Epilepsia* 47 (4), 704–716.
- Ragona, F., 2011. Cognitive development in children with Dravet syndrome. *Epilepsia* 52 (Suppl. 2), 39–43.
- Reichel, J.M., Nissel, S., Rogel-Salazar, G., Mederer, A., Kafer, K., Bedenk, B.T., Martens, H., Anders, R., Grosche, J., Michalski, D., Hartig, W., Wotjak, C.T., 2014. Distinct behavioral consequences of short-term and prolonged GABAergic depletion in prefrontal cortex and dorsal hippocampus. *Front. Behav. Neurosci.* 8, 452.
- Reid, A.Y., Pittman, Q.J., Teskey, G.C., 2012. A prolonged experimental febrile seizure results in motor map reorganization in adulthood. *Neurobiol. Dis.* 45 (2), 692–700.
- Rich, S.S., Annegers, J.F., Hauser, W.A., Anderson, V.E., 1987. Complex segregation analysis of febrile convulsions. *Am. J. Hum. Genet.* 41 (2), 249–257.
- Rubinstein, M., Westenbroek, R.E., Yu, F.H., Jones, C.J., Scheuer, T., Catterall, W.A., 2015. Genetic background modulates impaired excitability of inhibitory neurons in a mouse model of Dravet syndrome. *Neurobiol. Dis.* 73, 106–117.
- Sawyer, N.T., Helvig, A.W., Makinson, C.D., Decker, M.J., Neigh, G.N., Escayg, A., 2016. *Scn1a* dysfunction alters behavior but not the effect of stress on seizure response. *Genes Brain Behav.* 15 (3), 335–347.
- Scharfman, H.E., 2007. The CA3 “backprojection” to the dentate gyrus. *Prog. Brain Res.* 163, 627–637.
- Scheffer, I.E., Berkovic, S.F., 1997. Generalized epilepsy with febrile seizures plus. A genetic disorder with heterogeneous clinical phenotypes. *Brain* 120 (Pt 3), 479–490.
- Scott, R.C., Gadian, D.G., King, M.D., Chong, W.K., Cox, T.C., Neville, B.G., Connelly, A., 2002. Magnetic resonance imaging findings within 5 days of status epilepticus in childhood. *Brain* 125 (Pt 9), 1951–1959.
- Scott, R.C., King, M.D., Gadian, D.G., Neville, B.G., Connelly, A., 2003. Hippocampal abnormalities after prolonged febrile convulsion: a longitudinal MRI study. *Brain* 126 (Pt 11), 2551–2557.
- Shinnar, S., Glauser, T.A., 2002. Febrile seizures. *J. Child Neurol.* 17 (Suppl. 1), S44–S52.
- Shinnar, S., Bello, J.A., Chan, S., Hesdorffer, D.C., Lewis, D.V., Macfall, J., Pellock, J.M., Nordli, D.R., Frank, L.M., Moshe, S.L., Gomes, W., Shinnar, R.C., Sun, S., 2012. MRI abnormalities following febrile status epilepticus in children: the FEBSTAT study. *Neurology* 79 (9), 871–877.
- Tan, E.H., Yusoff, A.A., Abdullah, J.M., Razak, S.A., 2012. Generalized epilepsy with febrile seizure plus (GEFS+) spectrum: novel de novo mutation of *SCN1A* detected in a Malaysian patient. *J. Pediatr. Neurosci.* 7 (2), 123–125.
- Toth, Z., Yan, X.X., Haftoglou, S., Ribak, C.E., Baram, T.Z., 1998. Seizure-induced neuronal injury: vulnerability to febrile seizures in an immature rat model. *J. Neurosci.* 18 (11), 4285–4294.
- Tsuboi, T., 1987. Genetic analysis of febrile convulsions: twin and family studies. *Hum. Genet.* 75 (1), 7–14.
- Tsuboi, T., Endo, S., 1991. Genetic studies of febrile convulsions: analysis of twin and family data. *Epilepsy Res. Suppl.* 4, 119–128.
- Verity, C.M., Butler, N.R., Golding, J., 1985. Febrile convulsions in a national cohort followed up from birth. II – medical history and intellectual ability at 5 years of age. *Br. Med. J. (Clin. Res. Ed.)* 290 (6478), 1311–1315.
- Wang, Y.Y., Qin, J., Han, Y., Cai, J., Xing, G.G., 2011. Hyperthermia induces epileptiform discharges in cultured rat cortical neurons. *Brain Res.* 1417, 87–102.

- Ware, W.B., Ferron, J.M., Miller, B.M., 2012. *Introductory Statistics: A Conceptual Approach Using R*. Routledge.
- Wolff, M., Casse-Perrot, C., Dravet, C., 2006. Severe myoclonic epilepsy of infants (Dravet syndrome): natural history and neuropsychological findings. *Epilepsia* 47 (Suppl. 2), 45–48.
- Xiong, Y., Zhou, H., Zhang, L., 2014. Influences of hyperthermia-induced seizures on learning, memory and phosphorylative state of CaMKIIalpha in rat hippocampus. *Brain Res.* 1557, 190–200.
- Yu, F.H., Mantegazza, M., Westenbroek, R.E., Robbins, C.A., Kalume, F., Burton, K.A., Spain, W.J., McKnight, G.S., Scheuer, T., Catterall, W.A., 2006. Reduced sodium current in GABAergic interneurons in a mouse model of severe myoclonic epilepsy in infancy. *Nat. Neurosci.* 9 (9), 1142–1149.
- Yu, L.M., Polygalov, D., Wintzer, M.E., Chiang, M.C., McHugh, T.J., 2016. CA3 synaptic silencing attenuates kainic acid-induced seizures and hippocampal network oscillations. *eNeuro* 3 (1).